Polym. Bull. (2012) 69:439–454
DOI 10.1007/s00289-012-0740-z

ORIGINAL PAPER

Synthesis and photovoltaic properties of 1-(2,6-diisopropylphenyl)-2,5-di(2-thienyl)pyrrole-based low-bandgap polymers

**Vellaiappillai Tamilavan · Myungkwan Song ·
Tae-Won Ban · Sung-Ho Jin · Myung Ho Hyun**

Received: 17 January 2012 / Revised: 5 March 2012 / Accepted: 10 March 2012 /

Abstract Two new low-bandgap copolymers containing 1-(2,6-diisopropylphenyl)-2,5-di(2-thienyl)pyrrole, 2,1,3-benzothiadiazole and indenofluorene or fluorene (**PTPTIFB** and **PTPTFB**, respectively) were synthesized and characterized. The absorption spectrum of the polymer **PTPTIFB** covers the region from 300 to 750 nm, whereas polymer **PTPTFB** shows the absorption band up to 975 nm. The electrochemical bandgaps of the polymers were calculated to be 1.67 and 1.57 eV, respectively. The bulk heterojunction solar cells were fabricated with the configuration of ITO/PEDOT:PSS/**PTPTIFB** or **PTPTFB**:$PC_{70}BM$ (1:3 or 1:4 or 1:5 wt%)/TiO_x/Al, and the best performance was obtained with the blend of polymer:$PC_{70}BM$ (1:5 wt%) as an active layer. The device made from **PTPTIFB** showed the highest power conversion efficiency (PCE) of 1.18 %, while the device made from **PTPTFB** showed the PCE of 0.90 % measured using AM 1.5 G solar simulator at 100 mW cm^{-2} light illumination.

Keywords 1-(2,6-Diisopropylphenyl)-2,5-di(2-thienyl)pyrrole · Copolymers · Bulk heterojunction solar cells · Fluorene · Indenofluorene

Introduction

The development of broad absorbing polymers having extended delocalized π-electrons has been crucial, because of their potential application to the fabrication

---

V. Tamilavan · M. H. Hyun (✉)
Department of Chemistry, Chemistry Institute for Functional Materials, Pusan National University, Busan 690-735, Republic of Korea
e-mail: mhhyun@pusan.ac.kr

M. Song · T.-W. Ban · S.-H. Jin
Department of Chemistry Education and Interdisciplinary Program of Advanced Information and Display Materials, Pusan National University, Busan 609-735, Korea

of flexible large-area devices in polymer solar cells based on the bulk heterojunction (BHJ) model [1–5]. In BHJ solar cells, the interpenetrating network of electron donor (π-conjugated polymer) and electron acceptor ($PC_{60}BM$ or $PC_{70}BM$) layer is used for light harvesting and charge separation. The blends of low-bandgap π-conjugated polymers and $PC_{70}BM$ demonstrated promising power conversion efficiency (PCE) up to 7.4 % [6–25]. The PCE of the BHJ solar cell device has been correlated with four important factors, (1) light harvesting efficiency, (2) charge diffusion efficiency to donor–acceptor (D–A) interface, (3) charge separation efficiency at D–A interface, and (4) charge collection efficiency at the respective electrodes [26]. At present time, the major limiting factor to achieve higher PCE is the light harvesting ability of the donor polymer and the charge separation at D–A interface of the BHJ solar cell devices. In order to enhance the light harvesting ability of donor polymers it is essential to synthesize a polymer having broader absorption with high molar absorption coefficient. So far, the broad absorbing polymers were synthesized by copolymerizing the electron-rich and electron-deficient units in alternate fashion, and thereby broader absorption resulted from the combined electronic transitions such as π–π^* electronic transition and internal charge transfer (ICT) between the donor and acceptor moiety [27]. In other hand, we can improve the charge separation at D–A interfaces by using the polymer having appropriate energy levels and balanced charge carrier mobility, and also by making the quality of heterojunction between the donor and acceptor. According to literatures, fluorene and indenofluorene-based polymers have shown balanced charge carrier mobility when they applied to solar cell applications [28–35]. In addition, the effective charge separation at D–A interface was found when the donor polymer conduction band positioned minimum of 0.2–0.3 eV above the conduction band of $PC_{70}BM$ [36].

In our laboratory, we have been interested in the preparation of 1-(2,6-diisopropylphenyl)-2,5-di(2-thienyl)pyrrole (*N*-aryl TPT)-based π-conjugated polymers for BHJ solar cell applications [37–40]. Previously reported alternating copolymer containing *N*-aryl TPT unit and indenofluorene (**PTPTIF**) was found to show narrow absorption band in the range of 350–520 nm, and the photovoltaic studies showed maximum PCE of 1.12 % with J_{sc} of 3.39 mA cm^{-2}, V_{oc} of 0.67 V, FF of 49.31 % [37]. Some of the other *N*-aryl TPT copolymers incorporating phenylene (**PPTPT**) or thiophene (**PTTPT**) showed slightly broader absorption band (350–650 nm) with improved J_{sc} (7.41 mA cm^{-2}), PCE (1.35 %), and decreased FF (33 %) in their photovoltaic studies [38]. Whereas, interestingly the polymer (**PTPTTBT)** comprising *N*-aryl TPT as electron rich unit and thiophene-benzothiadiazole-thiophene (TBT) as electron acceptor unit showed quite broad and flat absorption band from 300 to 650 nm, and the photovoltaic studies showed maximum PCE of 1.57 % with high J_{sc} of 8.17 mA cm^{-2}, V_{oc} of 0.52 V, and FF of 36 % [39]. The photovoltaic studies of the *N*-aryl TPT polymers clearly suggest that broadening the absorption of *N*-aryl TPT polymer enhances the light harvesting and, consequently, improves the J_{sc} and PCE. Except for **PTPTIF** copolymer, all other *N*-aryl TPT polymers showed lower fill factor with high current density and PCE in their photovoltaic studies. The J_{sc} and FF are correlated with light harvesting ability and charge carrier mobility of the polymers. We expect that the higher FF obtained from the device made from **PTPTIF** is mainly attributed to the better carrier mobility of the polymer. In fact, fluorene and indenofluorene have identical properties and they are known to be good candidates for balanced charge carrier mobility [28–35, 41, 42]. Previously, copolymers consisting of repeating units of other two individual polymers, which were used as the electron donating materials in the ternary blend solar cell system, were reported to show good performance as the electron donating materials in the binary blend solar cell system [12]. In this instance, copolymers consisting of *N*-aryl TPT unit, indenofluorene and benzothiadiazole would be interesting.

In this continuity, in this study, we copolymerized *N*-aryl TPT unit with indenofluorene or fluorene and 2,1,3-benzothiadiazole with the aim of making new low-bandgap polymers having better carrier mobility. We believe that the presence of 2,1,3-benzothiadiazole (electron-deficient moiety) in polymer main chain extends the absorption spectrum up to the low energy part of the solar spectrum, and at the same time the presence of indenofluorene or fluorene in polymer main chain maintains the carrier mobility of the polymers. In this article, we report the synthesis, optoelectrical, and photovoltaic properties of the two new *N*-aryl TPT-based random copolymers.

Experimental section

Materials and general procedure

All reagents were purchased from Aldrich or TCI chemicals and used without further purification. Solvents were purified by using normal procedure and handled in a moisture-free atmosphere. Flash column chromatography was performed using silica gel (Merck Kieselgel 60, 70–230 mesh). Varian Mercury plus 300 spectrometer was employed for ^{1}H (300 MHz) and ^{13}C (75 MHz) NMR analysis and the chemical shifts were recorded in ppm units with chloroform as the internal standard. The solution and film state absorption studies were performed on JASCO V-570 spectrophotometers. Thermogravimetric analysis was done under N_2 atmosphere using a Mettler Toledo TGA/SDTA 851 analyzer at a heating rate of 10 °C min^{-1}. The CV analysis was performed on a CH Instruments Electrochemical Analyzer. The molecular weight and polydispersity of the polymer were determined by gel permeation chromatography (GPC) using a PLgel 5 μm MIXED-C column on an Agilent 1100 series liquid chromatography system with THF as an eluent. The GPC system performance was verified with polystyrene standard.

Device fabrication

The polymer bulk heterojunction solar cells were constructed as follows. The transparent ITO electrode (80 nm thick, 20 Ω/sq sheet resistance) was coated on glass substrates and cleaned by ultrasonication sequentially in detergent, deionized water, acetone, and isopropyl alcohol. After drying the substrates, a 40-nm thick layer of poly(3,4-ethylenedioxythiophene):poly(styrenesulfonate) (PEDOT:PSS)

(CLEVIOUS, PH500) was spin-coated onto the pre-cleaned and UV-ozone treated ITO substrates and baked in air at 150 °C for 30 min. Subsequently, the 80 nm thickness of active layer (Polymer: $PC_{70}BM$ blend solution) was spin-coated onto the ITO/PEDOT:PSS substrates. The Polymer:$PC_{70}BM$ blend solution was prepared by mixing each of the polymers and $PC_{70}BM$ solution in a weight ratio of 1:3, 1:4, or 1:5 wt% in 1,2-dichlorobenzene and chloroform (1:1 wt%). After drying the solvent, the 10 nm thickness of TiO_x precursor solution (1 wt%) was spin-coated (4,000 rpm) onto the active layer and subjected to heating at 80 °C for 10 min in air. After being subjected to a vacuum (5×10^{-6} Torr), an Al electrode with thickness of around 100 nm were deposited onto the TiO_x layer. Finally, the polymer bulk heterojunction solar cell devices were subjected to annealing at 100 °C for 30 min in a glove box. The top metal electrode area, comprising the active area of the solar cells, was found to be 4 mm^2. The bulk heterojunction solar cell device performance were measured using a AM 1.5 G solar simulator (Oriel 300 W) at 100 mW cm^{-2} light illumination after adjusting the light intensity using Oriel power meter (model no. 70260 which was calibrated using laboratory standards that are traceable to the National Institute of Standards and Technologies, USA). Current–voltage (*J*–*V*) characteristics of the photovoltaic cells were measured using a standard source measurement unit (Keithley 236). The external quantum efficiency (EQE) spectra of the solar cell devices were measured on ORIEL IQE 200™ instrument. All fabrication steps and characterization measurements were performed in an ambient environment without a protective atmosphere. The thickness of the thin films was measured using a KLA Tencor Alpha-step IQ surface profilometer with an accuracy of ±1 nm.

Synthesis of polymers

General procedure for polymerization: a solution of **1** (0.32 g, 0.5 mmol), **2** (0.073 g, 0.25 mmol), and **3** (0.22 g, 0.25 mmol) for polymer **PTPTIFB** or **1** (0.32 g, 0.5 mmol), **2** (0.073 g, 0.25 mmol), and **4** (0.14 g, 0.25 mmol) for polymer **PTPTFB** in THF (60 mL) was purged well with N_2 for 45 min and then $Pd(PPh_3)_4$ (0.03 g, 5 mol%) and aqueous 2 M K_2CO_3 solution (7 ml) were added. The whole mixture was refluxed with vigorous stirring under N_2. After 72 h, 50 mg of phenyl boronic acid was added and refluxed for 6 h and then 0.1 ml of bromobenzene were added and refluxed for another 6 h. The solvent was concentrated and cooled to RT. The cooled mixture was then poured into methanol:water mixture (200:100 ml) with vigorous stirring. The precipitate was recovered by filtration and washed well with 2 N HCl, and then the crude polymer was extracted with methanol for 24 h and acetone for 24 h in a Soxhlet apparatus. The residue was dissolved in THF and reprecipitated in methanol to afford a pure polymer. The NMR analysis of the synthesized polymers clearly indicates that the presence of all three monomers in polymer main chain at different ratio. The NMR spectrum was shown in Fig. 1. **PTPTIFB**: yield (0.35 g, 44%). ^1H NMR (300 MHz, CDCl3): δ 7.84 (s, 1H), 7.30–7.70 (m, 6H), 7.01 (d, 1H), 6.63–6.85 (m, 2H), 6.04–6.36 (m, 2H), 2.61 (s, 2H), 2.00 (s, 2H), 0.84–1.24 (m, 20H), 0.56-0.82 (m, 6H). **PTPTFB**: yield

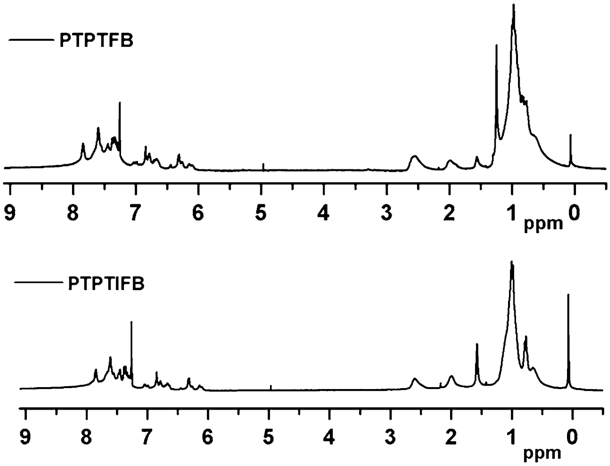

Fig. 1 ^{1}H NMR spectrums of the copolymer **PTPTIFB** and **PTPTFB**

(0.32 g, 49%). ^{1}H NMR (300 MHz, CDCl3): δ 7.84 (s, 2H), 7.30–7.70 (m, 10H), 6.60–7.1 (m, 5H), 6.04–6.36 (m, 2H), 2.58 (s, 2H), 2.00 (s, 1H), 0.50–1.24 (m, 20H).

Results and discussion

Synthesis and characterization

Synthetic approaches to the polymers are shown in Scheme 1. The electron donating *N*-aryl TPT monomer, 1-(2,6-diisopropylphenyl)-2,5-di(5-(4,4,5,5-tetramethyl-1,3,2-dioxaborolan-2-yl)-2-thienyl)pyrrole (**1**), was synthesized according to the procedure reported from our laboratory [37, 38]. The electron accepting monomer, 4,7-dibromo-2,1,3-benzothiadiazole (**2**) [43], and electron rich co-monomers **3** [37] and **4** [20, 23] were synthesized via the well known procedures. A Suzuki polymerization of monomers **1**, **2**, and **3** or monomers **1**, **2**, and **4** at the ratio of 2:1:1 was carried out in THF solution containing 5 mol% $Pd(PPh_3)_4$ and aqueous 2 M K_2CO_3 solution as catalyst. The resulting polymers were end capped by treating with bromobenzene and phenyl boronic acid to afford **PTPTIFB** and **PTPTFB**, respectively. From the NMR spectrum of **PTPTIFB**, the ratio of *N*-aryl TPT monomer and indenofluorene in the repeating unit "m" and the ratio of *N*-aryl TPT monomer and (2,1,3-benzothiadiazole) in the repeating unit "n" were analyzed to be 1:0.5 and 1:0.5, respectively. Similarly, from the NMR spectrum of **PTPTFB**, the ratio of *N*-aryl TPT monomer and fluorene in the repeating unit "m" and the ratio of *N*-aryl TPT monomer and (2,1,3-benzothiadiazole) in the repeating unit "n" to be 1:0.5 and 1:1, respectively. Both polymers **PTPTIFB** and **PTPTFB** show good solubility in chlorinated solvents, such as chloroform, chlorobenzene, and *o*-dichlorobenzene. The weight average molecular weight (M_w) of polymers **PTPTIFB** and **PTPTFB** were found to be 1.39×10^4 and 8.23×10^3 and their

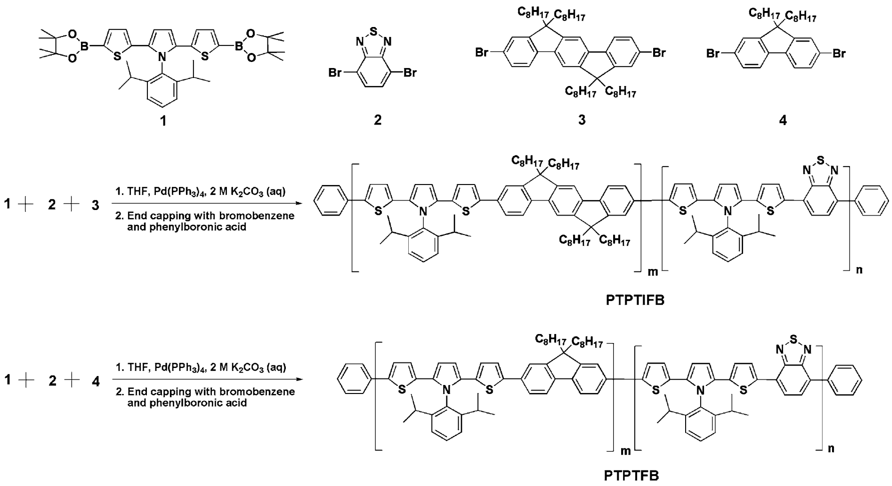

Scheme 1 Synthetic route for the synthesis of polymers **PTPTIFB** and **PTPTFB**

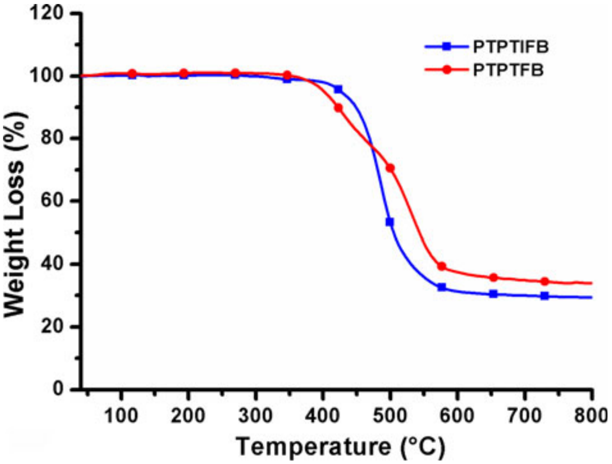

Fig. 2 TGA curve for polymers **PTPTIFB** and **PTPTFB**

polydispersities were 1.83 and 1.76, respectively, by GPC with polystyrene standards in tetrahydrofuran (THF). The TGA analysis suggested that both the polymers have excellent thermal stability with 5 % weight loss temperature of 430 and 400 °C, respectively. Figure 2 represents the TGA curves of the copolymers. The polymerization results and TGA data of the polymers are listed in Table 1.

Optical properties

The absorption data of the synthesized polymers are listed in Table 1. The normalized absorption spectra of **PTPTIFB** and **PTPTFB** were measured both in

Table 1 Polymerization results, thermal, optical, and electrochemical properties of **PTPTIFB** and **PTPTFB**

	PTPTIFB	PTPTFB
M_w^a	1.39×10^4	8.23×10^3
PDI[a]	1.83	1.76
TGA[b]	430	400
Abs (nm)		
Solution	416, 603	402, 593, 853
Film[c]	421, 607	403, 602, 857
HOMO (eV)[d]	−5.05	−5.00
LUMO (eV)[d]	−3.38	−3.43
E_g (eV)[e]	1.67	1.57
E_g (eV)[f]	1.69	1.63 (or) 1.27

[a] Weight average molecular weight (M_w) and polydispersity (PDI) of the polymers were determined by GPC using polystyrene standard

[b] 5% weight loss temperature measured by TGA under nitrogen gas

[c] Measurements in thin film were performed onto the quartz substrate

[d] The HOMO–LUMO level of the polymers were estimated from cyclic voltammetry analysis

[e] The electrochemical bandgap estimated from the cyclic voltammetry analysis

[f] The optical bandgap estimated from the onset wavelength of the optical absorption in thin film

solution (chloroform) and thin films on quartz (Fig. 3). As shown in Fig. 3, the absorption maxima of polymer **PTPTIFB** were found to be at 421 and 607 nm in film state and found to be at 416 and 603 nm in solution. The film state absorption spectrum is slightly red shifted (~5 nm) compared to the solution state absorption spectrum. In the case of **PTPTFB** the maximum absorption peaks appeared at 403, 602, and 857 nm in film and appeared at 402, 593 and 853 nm in solution. We expect that the peaks at high energy part of the solar spectrum (around 400 nm) are mainly attributed to the π–π^* electronic transitions of electron donor units such as *N*-aryl TPT, indenofluorene, or fluorene. In the other hand, the peaks at low energy part (around 600 nm) are attributed to the π–π^* electronic transitions of electron acceptor units including 2,1,3-benzothiadiazole. The polymers **PTPTIFB** and **PTPTFB** show quite similar absorption spectrum up to 750 nm, but **PTPTFB** shows additional weak absorption at NIR region. The additional absorption peak of **PTPTFB** at around 850 nm might be attributed to the internal charge transfer (ICT) between the electron donor (*N*-aryl TPT) and electron acceptor (2,1,3-benzothiadiazole) units. In the case of polymer **PTPTIFB**, four long-alkyl groups attached on polymer back bone might lead bond flexibility between the repeating units of **PTPTIFB** and, consequently, the internal charge transfer might be hindered and the peak at around 850 nm is not observed. The optical bandgaps of polymers **PTPTIFB** and **PTPTFB** were estimated from the onset wavelength of their film state absorption spectra to be 1.69 eV (onset wavelength: 733 nm) and 1.63 eV (onset wavelength: 760 nm) or 1.27 eV (onset wavelength: 976 nm), respectively. The reported optical bandgap of **PTPTIF** was 2.36 eV [37]. The bandgaps of newly

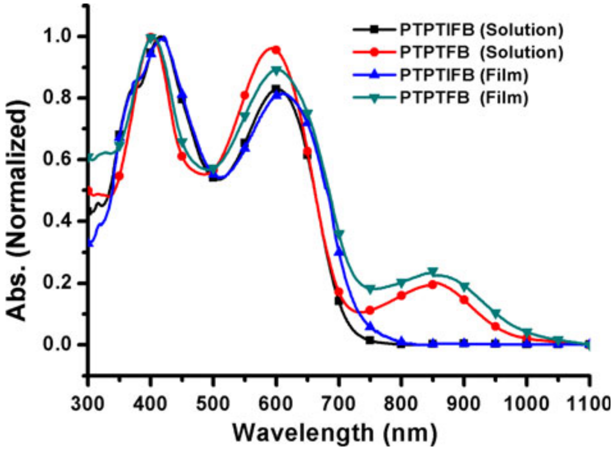

Fig. 3 UV–Visible absorption spectra of polymers **PTPTIFB** and **PTPTFB** in chloroform solution and thin film

synthesized polymers were found to be significantly reduced compared to that of polymer **PTPTIF** [37]. The incorporation of the electron acceptor (benzothiadiazole) moiety in polymer main chain is expected to reduce the bandgaps of the polymers.

Electrochemical properties

The energy levels [highest occupied molecular orbital (HOMO) and lowest unoccupied molecular orbital (LUMO)] of polymers **PTPTIFB** and **PTPTFB** were determined using cyclic voltammetry (CV) analysis. Cyclic voltammetry (CV) experiments were conducted on a drop-cast polymer film on a platinum working electrode in acetonitrile containing 0.1 M tetrabutylammonium tetrafluoroborate (TBATFB) as the supporting electrolyte at room temperature and ambient atmosphere at a scan rate of 100 mV/s. Ag/AgCl and platinum wire were used as the reference and counter electrode, respectively. The performance of the CV instrument was calibrated using the ferrocene/ferrocenium (FOC) redox couple as an internal standard before and after the analysis. Figure 4 represents the cyclic voltamogram of polymers **PTPTIFB** and **PTPTFB**. The energy levels of the polymers were calculated according to the following equation [44, 45]: $E_{\mathrm{HOMO}} = [-(\mathrm{E}_{\mathrm{ox,onset\ vs.\ Ag/AgCl}} - E_{\mathrm{onset,ferrocene\ vs.\ Ag/AgCl}}) - 4.8]$ eV and $E_{\mathrm{LUMO}} = [-(E_{\mathrm{red,onset\ vs.\ Ag/AgCl}} - E_{\mathrm{onset,ferrocene\ vs.\ Ag/AgCl}}) - 4.8]$ eV, where 4.8 eV is the energy level of ferrocene below the vacuum level and $E_{\mathrm{(onset\ ferrocene\ vs.\ Ag/AgCl)}}$ is 0.51 eV and $E_{\mathrm{ox,onset}}$ and $E_{\mathrm{red,onset}}$ are the onset potential values in volts for oxidation and reduction processes against Ag/AgCl reference electrode. From the CV analysis, the onset oxidation ($E_{\mathrm{ox,onset}}$) potentials of polymers **PTPTIFB** and **PTPTFB** were determined to be 0.76 and 0.71 V, respectively, and the HOMO energy levels were calculated to be −5.05 and −5.00 eV, respectively. The onset

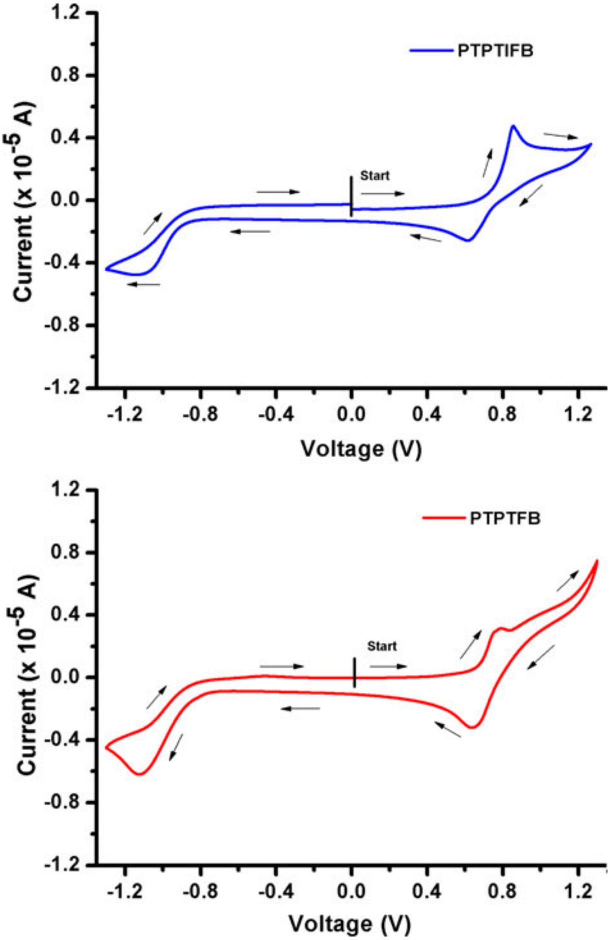

Fig. 4 Cyclic voltammograms of **PTPTIFB** and **PTPTFB** films cast on platinum working electrode in 0.1 M TBATFB/acetonitrile at 100 mV/s, potential versus Fe/Fe$^+$

reduction potentials ($E_{\text{red,onset}}$) of polymers **PTPTIFB** and **PTPTFB** were estimated to be −0.91 and −0.86 V, respectively, and the LUMO energy levels of polymers were calculated to be −3.38 and −3.43 eV, respectively. The electrochemical bandgaps calculated from the HOMO–LUMO levels of polymers **PTPTIFB** and **PTPTFB** were 1.67 and 1.57 eV, respectively. The electrochemical bandgaps of polymers **PTPTIFB** and **PTPTFB** are correlated well with the optical bandgaps of the polymers (1.69 and 1.63 eV, respectively) calculated from the onset wavelength of the absorption. The electrochemical properties of the polymers are included in Table 1. The energy levels of the polymers and $PC_{70}BM$ with all other materials used in BHJ solar cells fabrication are illustrated in Fig. 5. The LUMO energy levels of polymers **PTPTIFB** and **PTPTFB** were located above the $PC_{70}BM$ LUMO level. In this instance, the efficient electron transfer from the conduction

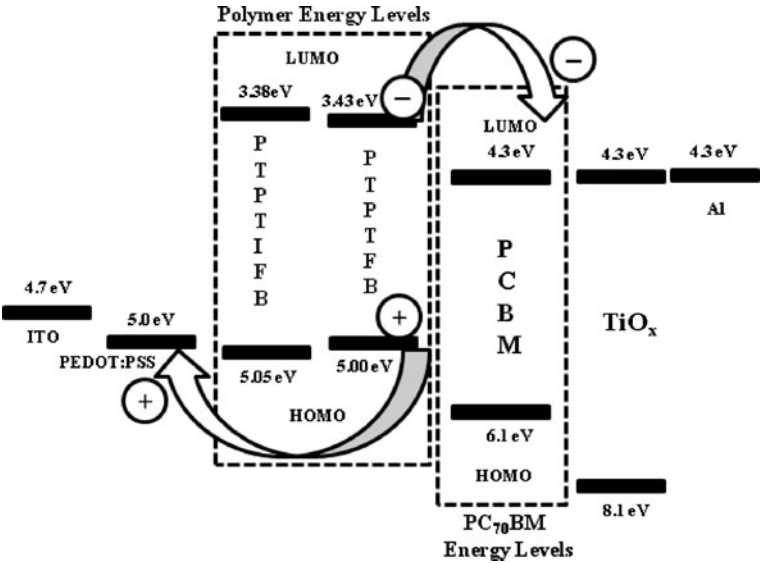

Fig. 5 The energy level diagram of polymers **PTPTIFB**, **PTPTFB**, and **PC$_{70}$BM** with all other materials used in BHJ solar cell

band of the donor (polymer) to the conduction band of the acceptor (PC$_{70}$BM), which is essential for the charge separation of the excitones, is insured.

Photovoltaic properties

The bulk heterojunction solar cell devices were fabricated with a structure of ITO (80 nm)/PEDOT:PSS (40 nm)/polymer:PC$_{70}$BM (1:3 or 1:4 or 1:5 wt% of 80 nm layer)/TiO$_x$ (10)/Al (100 nm). In this device structure ITO and Al were used as the hole and electron-collecting electrodes. PEDOT:PSS and TiO$_x$ were used as the hole transporting and hole blocking as well as electron transporting layers. The J–V characteristics of devices measured under the illumination of AM 1.5 G (100 mW cm^{-2}) from a solar simulator are shown in Fig. 6 and the detailed results are summarized in Table 2. In this study we made three devices for each polymer with 1:3, 1:4, and 1:5 wt% ratio of the polymer and PC$_{70}$BM in the active layer. In every case, the PCE of the device made from 1:5 wt% (polymer:PC$_{70}$BM) is higher than that of the device made from 1:3 wt% (polymer:PC$_{70}$BM) or 1:4 wt% (polymer:PC$_{70}$BM) measured under the identical condition. In the case of polymer **PTPTIFB**, the maximum power conversion efficiency (PCE) was 1.18 % with a open-circuit voltage (V_{oc}) of 0.43 V, a short-circuit current density (J_{sc}) of 7.28 mA cm^{-2}, and a fill factor (FF) of 37.82 %, and polymer **PTPTFB** showed maximum PCE of 0.90 % with a V_{oc} of 0.36 V, a J_{sc} of 6.74 mA cm^{-2}, and a FF of 37.17 %. The device containing **PTPTIFB**:PC$_{70}$BM (1:4 wt%) and **PTPTIFB**:PC$_{70}$BM (1:3 wt%) as an active layer showed PCE of 0.95% (V_{oc} = 0.40 V, J_{sc} = 6.79 mA cm^{-2}, and FF = 34.65 %) and

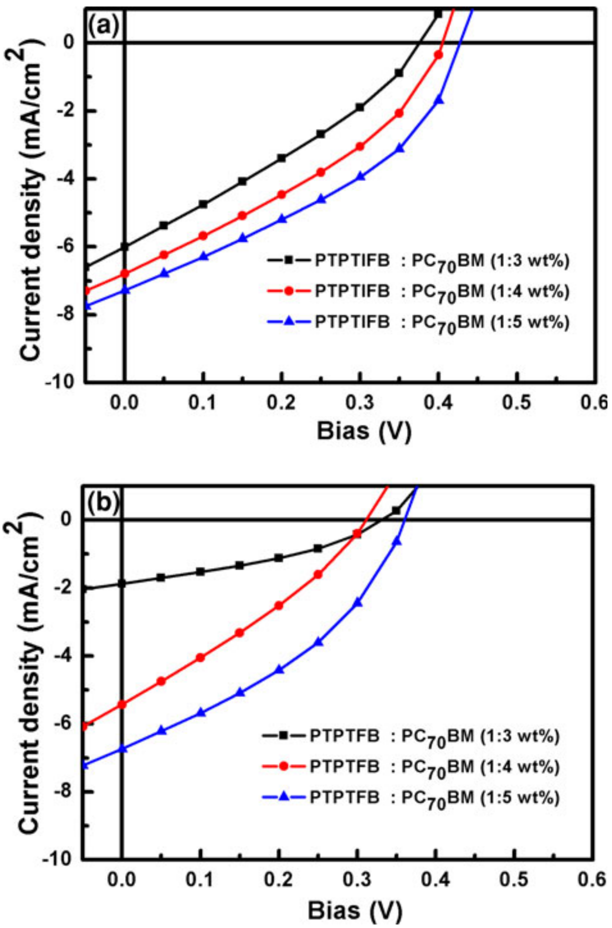

Fig. 6 *J*–*V* characteristics of BHJ solar cells prepared from ITO/PEDOT:PSS/**PTPTIFB** or **PTPTFB**:$PC_{70}BM/TiO_X/Al$ under AM 1.5 irradiation (100 mW/cm^2)

Table 2 Solar cell performance of **PTPTIFB** and **PTPTFB** as electron donor with $PC_{70}BM$ as an electron acceptor in ITO/PEDOT:PSS/**PTPTIFB** or **PTPTFB**:$PC_{70}BM/TiO_X/Al$ device

Active layer (wt%)	V_{oc} (V)	J_{sc} (mA/cm^2)	FF (%)	PCE (%)
PTPTIFB: $PC_{70}BM$ (1:3)	0.38	6.00	29.82	0.68
PTPTIFB: $PC_{70}BM$ (1:4)	0.40	6.79	34.65	0.95
PTPTIFB: **$PC_{70}BM$** (1:5)	0.43	7.28	37.82	1.18
PTPTFB: $PC_{70}BM$ (1:3)	0.33	1.87	35.65	0.22
PTPTFB: $PC_{70}BM$ (1:4)	0.31	5.43	29.94	0.50
PTPTFB: $PC_{70}BM$ (1:5)	0.36	6.74	37.17	0.90

V_{oc} open-circuit voltage, J_{sc} short-circuit current density, *FF* fill factor, *PCE* power conversion efficiency

0.68 % (V_{oc} = 0.38 V, J_{sc} = 6.00 mA cm^{-2}, FF = 29.82%), respectively, while the device containing **PTPTFB**:PC$_{70}$BM (1:4 wt%) and **PTPTFB**:PC$_{70}$BM (1:3 wt%) as an active layer showed PCE 0.50 % (V_{oc} = 0.31 V, J_{sc} = 5.43 mA cm^{-2}, and FF = 29.94 %) and 0.22 % (V_{oc} = 0.33 V, J_{sc} = 1.87 mA cm^{-2}, and FF = 35.65 %), respectively. The higher content of PC$_{70}$BM is expected to be more favorable for the efficient light harvesting and electron–hole separation. With increasing the PC$_{70}$BM content, the J_{sc} increases for both polymer devices. By increasing the PC$_{70}$BM content, the charge separation is expected to increase. The current density (J_{sc}) and open-circuit voltage (V_{oc}) of the device made form **PTPTIFB** was found to be slightly higher than those of the device made from **PTPTFB**. The V_{oc} is the energy difference between the HOMO level of the polymer and the LUMO level of the PC$_{70}$BM [46]. Consequently, the deeper HOMO level of polymer **PTPTIFB** compared to the HOMO energy level of **PTPTFB** might be responsible for the higher V_{oc} of the devices made from **PTPTIFB**. The higher J_{sc} value observed on the device made from **PTPTIFB**:PC$_{70}$BM compared to that on the device made from **PTPTFB**:PC$_{70}$BM under the identical experimental condition is expected to be originated from the higher molecular weight of polymer **PTPTIFB**. The high molecular weight polymers have been reported to show higher J_{sc} and PCE values than the low molecular weight polymers under identical condition [47, 48]. The fill factor values of the devices made from both polymers are almost identical, indicating both polymers have similar carrier mobility. The overall photovoltaic performances of the polymers **PTPTIFB** and **PTPTFB** were found to be quite similar with the known polymer **PTPTIF**. But, the current densities (J_{sc}) of the photovoltaic devices containing the newly synthesized polymers as a donor polymer were found to be two times higher than that of the device containing known polymer, **PTPTIF**, (J_{sc} = 3.39 mA cm^{-2}) [37]. As we mentioned in introduction, the broad absorption band of the polymers (**PTPTIFB** and **PTPTFB)** are responsible for the higher J_{sc} values. At the same time, the fill factors (FF) of the photovoltaic devices containing **PTPTIFB** or **PTPTFB** were found to be lower than that of **PTPTIF** polymer**-**based device (FF = 49%), but slightly higher than other *N*-aryl TPT-based polymer devices (FF = 33%), which do not contain indenofluorene or fluorene [38, 39]. From these results, we expect that the presence of indenofluorene or fluorene in polymer main chain somewhat maintain the carrier mobility of the polymers and offered the better fill factor (FF) values. Figure 7 shows the EQE spectra of the BHJ solar cell devices prepared using **PTPTIFB**:PC$_{70}$BM (1:5 wt%) and **PTPTFB**:PC$_{70}$BM (1:5 wt%) as an active layer. The EQE spectra are consistent with the film state absorption spectra of polymer:PC$_{70}$BM (1:5 wt%) blend as shown in Fig. 7. Each of the polymer devices showed a very broad photoresponse range covering from 300 to 750 nm. The photoresponse of **PTPTIFB-**based solar cell device was found to be higher in the range of 300–500 nm and slightly lower in the range of 500–750 nm compared to that of **PTPTFB-**based solar cell device.

The surface morphology of the active layer was studied by using atomic force microscope (AFM) analysis. Figure 8 shows the AFM images of the blends of **PTPTIFB**:PC$_{70}$BM (1:5 wt%) and **PTPTFB**:PC$_{70}$BM (1:5 wt%). Their surfaces are quite smooth and the root-mean-square (rms) roughnesses were found to be 1.04 and 1.60 nm, respectively.

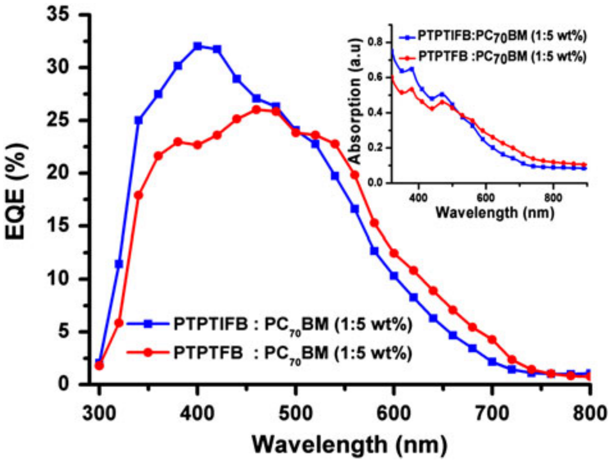

Fig. 7 EQE spectra of the BHJ solar cells prepared from **PTPTIFB**:PC$_{70}$BM (1:5 wt%) and **PTPTFB**:PC$_{70}$BM (1:5 wt%) as active layers. *Inset* the absorption spectra of the **PTPTIFB**:PC$_{70}$BM (1:5 wt%) and **PTPTFB**:PC$_{70}$BM (1:5 wt%) blend film

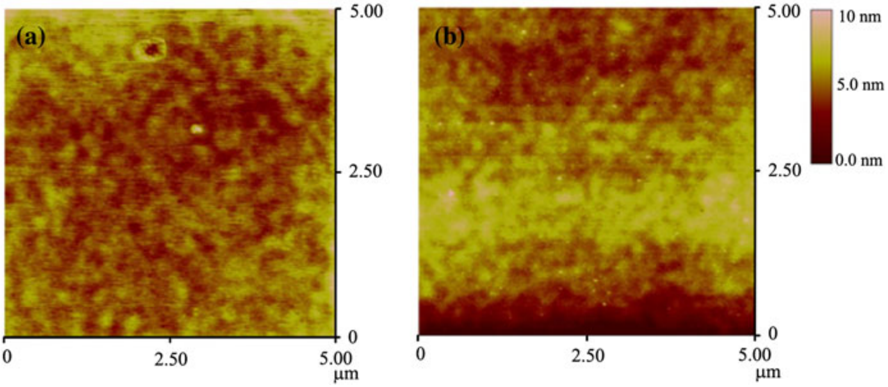

Fig. 8 AFM image obtained by tapping-mode on the surface for **PTPTIFB**:PC$_{70}$BM (1:5 wt%) (**a**) and **PTPTFB**:PC$_{70}$BM (1:5 wt%) (**b**) spin-coated thin film

Conclusions

In this study, we successfully synthesized two new *N*-aryl TPT-based broad absorbing low-bandgap random copolymers such as **PTPTIFB** and **PTPTFB** via Suzuki polycondensation reaction. Both polymers, **PTPTIFB** and **PTPTFB**, showed strong absorption band in the visible part of solar spectrum. The electrochemical bandgaps of the polymers were found to be 1.67 and 1.57 eV, respectively, and the HOMO and LUMO energy levels were also found to be suitable for BHJ solar cell applications. The photovoltaic properties of the polymers were studied by using devices with a configuration of ITO/PEDOT:PSS/polymer:PC$_{70}$BM/TiO$_x$/Al. The device made from the blend of **PTPTIFB**:$PC_{70}BM$ (1:5 wt%) showed highest PCE of 1.18 % ($V_{oc} = 0.43$ V, $J_{sc} = 7.28$ mA cm^{-2}, and FF = 37.82 %) while the device made from the blend of **PTPTFB**:$PC_{70}BM$ (1:5 wt%) showed slightly lower PCE of 0.90 % ($V_{oc} = 0.36$ V, $J_{sc} = 6.74$ mA cm^{-2}, and FF = 37.17%). The comparison studies of the newly synthesized polymers with previously reported *N*-aryl TPT polymers clearly indicates that broadening the absorption band of polymers enhances the current density of the BHJ solar cell devices. In addition, we concluded that the presence of indenofluorene or fluorene in *N*-aryl TPT-based polymer main chain slightly increases the fill factor of the *N*-aryl TPT-based polymer BHJ solar cell devices.

Acknowledgments This research was supported by the New & Renewable Energy program of the Korea Institute of Energy Technology Evaluation and Planning (KETEP) grant (no. 20103020010050) funded by the Ministry of Knowledge Economy, Republic of Korea.

References

1. Chang JA, Rhee JH, Im SH, Lee YH, Kim HJ, Seok SI, Nazeeruddin MK, Gratzel M (2010) High-performance nanostructured inorganic-organic heterojunction solar cells. Nano Lett 10:2609
2. Gadisa A, Mammo W, Andersson LM, Admassie S, Zhang F, Andersson MR, Inganas O (2007) A new donor–acceptor–donor polyfluorene copolymer with balanced electron and hole mobility. Adv Funct Mater 17:383
3. Lee JH, Cho S, Roy A, Jung HT, Heeger AJ (2010) Enhanced diode characteristics of organic solar cells using titanium suboxide electron transport layer. Appl Phys Lett 96:1633031
4. Ayzner AL, Wanger DD, Tassone CJ, Tolbert SH, Schwartz BJJ (2008) Room to improve conjugated polymer-based solar cells: understanding how thermal annealing affects the fullerene component of a bulk heterojunction photovoltaic device. Phys Chem C 112:18711
5. Gunes S, Neugebauer H, Sariciftci NS (2007) Conjugated polymer-based organic solar cells. Chem Rev 107:1324
6. Chen HY, Hou J, Zhang S, Liang Y, Yang G, Yang Y, Yu L, Wu Y, Li G (2009) Polymer solar cells with enhanced open-circuit voltage and efficiency. Nat Photon 3:649
7. Liang Y, Xu Z, Xia J, Tsai ST, Wu Y, Li G, Ray C, Yu L (2010) For the bright future-bulk heterojunction polymer solar cells with power conversion efficiency of 7.4%. Adv Mater 22:1
8. Chu TA, Lu J, Beaupre S, Zhang Y, Pouliot JR, Wakim S, Zhou J, Leclerc M, Li Z, Ding J, Tao Y (2011) Bulk heterojunction solar cells using thieno[3,4-c]pyrrole-4,6-dione and dithieno[3,2-b:20,30-d]silole copolymer with a power conversion efficiency of 7.3%. J Am Chem Soc 133:4250
9. Price SC, Stuart AC, Yang L, Zhou H, You W (2011) Fluorine substituted conjugated polymer of medium band gap yields 7% efficiency in polymer-fullerene solar cells. J Am Chem Soc 133:4625
10. Son HJ, Wang W, Xu T, Liang Y, Wu Y, Li G, Yu L (2011) Synthesis of fluorinated polythienothiophene-*co*-benzodithiophenes and effect of fluorination on the photovoltaic properties. J Am Chem Soc 133:1885
11. Park SH, Roy A, Beaupre S, Cho S, Coates N, Moon JS, Moses D, Leclerc M, Lee K, Heeger AJ (2009) Bulk heterojunction solar cells with internal quantum efficiency approaching 100%. Nat Photon 3:297
12. Park SJ, Cho JM, Byun WB, Lee JC, Shin WS, Kang IN, Moon SJ, Lee SK (2011) Bulk heterojunction polymer solar cells based on binary and ternary blend systems. J Poly Sci A 49:4416
13. Lee SK, Cho S, Tong M, Seo JH, Heeger AJ (2011) Effects of substituted side-chain position on donor–acceptor conjugated copolymers. J Poly Sci A 49:1821
14. Liang Y, Yu L (2010) A new class of semiconducting polymers for bulk heterojunction solar cells with exceptionally high performance. Acc Chem Res 43:1227
15. Piliego C, Holcombe TW, Douglas JD, Woo CH, Beaujuge PM, Frechet JMJ (2010) Synthetic control of structural order in *N*-alkylthieno[3,4-c]pyrrole-4,6-dione-based polymers for efficient solar cells. J Am Chem Soc 132:7595
16. Zheng Q, Jung BJ, Sun J, Katz HE (2010) Ladder-type oligo-π-phenylene-containing copolymers with high open-circuit voltages and ambient photovoltaic activity. J Am Chem Soc 132:5394

17. Lunt RR, Osedach TP, Brown PR, Rowehl JA, Bulovic V (2011) Practical roadmap and limits to nanostructured photovoltaics. Adv Mater 23:5712
18. Huo L, Hou J (2011) Benzo[1,2-b:4,5-b']dithiophene-based conjugated polymers: band gap and energy level control and their application in polymer solar cells. Polym Chem 2:2453
19. Brabe CJ, Gowrisanker S, Halls JJM, Laird D, Jia S, Williams SP (2010) Polymer-fullerene bulk-heterojunction solar cells. Adv Mater 22:3839
20. Inganas O, Zhang F, Tvingstedt K, Andersson LM, Hellstrom S, Andersson MR (2010) Polymer photovoltaics with alternating copolymer/fullerene blends and novel device architectures. Adv Mater 22:E100
21. Wang E, Hou L, Wang Z, Hellstrom S, Zhang F, Inganas O, Andersson MR (2010) An easily synthesized blue polymer for high-performance polymer solar cells. Adv Mater 22:1
22. Park HJ, Kang MG, Ahn SH, Guo LJ (2010) A facile route to polymer solar cells with optimum morphology readily applicable to a roll-to-roll process without sacrificing high device performance. Adv Mater 22:E247
23. Cheedarala RK, Kim GH, Cho S, Lee J, Kim J, Song HK, Kim JY, Yang C (2011) Ladder-type heteroacene polymers bearing carbazole and thiophene ring units and their use in field-effect transistors and photovoltaic cells. J Mater Chem 21:843
24. Kim J, Yun MH, Anant P, Cho S, Jacob J, Kim JY, Yang C (2011) Copolymers comprising 2,7-carbazole and bis-benzothiadiazole units for bulk-heterojunction solar cells. Chem Eur J 17:14681
25. Amb CM, Chen S, Graham KR, Subbiah J, Small CE, So F, Reynolds JR (2011) Dithienogermole as a fused electron donor in bulk heterojunction solar cell. J Am Chem Soc 133:10062
26. Boucle J, Ravirajan P, Nelson J (2007) Hybrid polymer–metal oxide thin films for photovoltaic applications. J Mater Chem 17:3141
27. Bundgaard E, Krebs FC (2007) Low band gap polymers for organic photovoltaics. Sol Energy Mater Sol Cells 91:954
28. Chen MH, Hou J, Hong Z, Yang G, Sista S, Chen LM, Yang Y (2009) Efficient polymer solar cells with thin active layers based on alternating polyfluorene copolymer/fullerene bulk heterojunctions. Adv Mater 21:4238
29. Inganas O, Zhang F, Andersson MR (2009) Alternating polyfluorenes collect solar light in polymer photovoltaics. Acc Chem Res 42:1731
30. Muller C, Wang E, Andersson LM, Tvingstedt K, Zhou Y, Andersson MR, Inganas O (2010) Influence of molecular weight on the performance of organic solar cells based on a fluorene derivative. Adv Func Mater 20:2124
31. Cheng YJ, Yang SH, Hsu CS (2009) Synthesis of conjugated polymers for organic solar cell applications. Chem Rev 109:5868
32. Kim H, Schulte N, Zhou G, Mullen K, Laquai F (2011) A high gain and high charge carrier mobility indenofluorene-phenanthrene copolymer for light amplification and organic lasing. Adv Mater 23:894
33. Kim J, Kim SH, Jung IH, Jeong E, Xia Y, Cho S, Hwang IW, Lee K, Suh H, Shim HK, Woo HY (2010) Synthesis and characterization of indeno[1,2-b]fluorene-based low bandgap copolymers for photovoltaic cells. J Mater Chem 20:1577
34. Duan C, Cai W, Zhong C, Li Y, Wang X, Huang F, Cao Y (2011) Bandgap engineering of indenofluorene-based conjugated copolymers with pendant donor-p-acceptor chromophores for photovoltaic applications. J Polym Sci Part A 49:4406
35. Usta H, Risko C, Wang Z, Huang H, Deliomeroglu MK, Zhukhovitskiy A, Facchetti A, Marks TJ (2009) Design, synthesis, and characterization of ladder-type molecules and polymers. Air-stable, solution-processable n-channel and ambipolar semiconductors for thin-film transistors via experiment and theory. J Am Chem Soc 131:5586
36. Zhu Z, Waller D, Gaudiana R, Morana M, Mulhlbacher D, Scharber M, Brabec C (2007) Panchromatic conjugated polymers containing alternating donor/acceptor units for photovoltaic applications. Macromolecules 40:1981
37. Tamilavan V, Sakthivel P, Li Y, Song M, Kim CH, Jin SH, Hyun MH (2010) Synthesis and characterization of indenofluorene-based copolymers containing 2, 5-bis(2-thienyl)-*N*-arylpyrrole for bulk heterojunction solar cells and polymer light-emitting diodes. J Polym Sci Part A 48:3169
38. Tamilavan V, Song M, Jin SH, Hyun MH (2010) Synthesis of three new 1-(2,6-Diisopropylphenyl)-2,5-di(2-thienyl) pyrrole-based donor polymers and their bulk heterojunction solar cell applications. J Polym Sci Part A 48:5514
39. Tamilavan V, Song M, Jin SH, Hyun MH (2011) Synthesis of conjugated polymers with broad absorption bands and photovoltaic properties as bulk heterojuction solar cells. Polymer 52:2384

40. Tamilavan V, Song M, Jin SH, Hyun MH (2011) Synthesis and photovoltaic properties of hetero-aromatic low-band gap oligomers for bulk heterojunction solar cells. Syn Metal 161:1199
41. Keivnidis PE, Jacob J, Oldridge L, Sonar P, Carbonnier B, Baluschev S, Grimsdale AC, Mullen K, Wegner G (2005) Photophysical characterization of light-emitting poly(indenofluorene)s. Chem Phys Chem 6:1650
42. Setayesh SD, Marsitzky D, Mullen K (2000) Bridging the gap between polyfluorene and ladder-poly-p-phenylene: synthesis and characterization of poly-2,8-indenofluorene. Macromolecules 33:2016
43. Mancilha F, Neto BAD, Lopes AS, Moreira PF Jr, Quina FH, Goncalves RS, Dupont J (2006) Are molecular 5,8-π-extended quinoxaline derivatives good chromophores for photoluminescence applications. Eur J Org Chem 21:4924–4933
44. Li KC, Hsu YC, Lin JT, Yang CC, Wei KH, Lin HC (2009) Soluble narrow-band-gap copolymers containing novel cyclopentadithiophene units for organic photovoltaic cell applications. J Polym Sci A 47:2073
45. Hsu SLC, Lin YC, Lee RF, Sivakumar C, Chen JS, Chou WY (2009) Synthesis and characterization of new low bandgap polyfluorene copolymers for bulk heterojunction solar cells. J Polym Sci A 47:5336
46. Dennler G, Scharber MC, Brabec C (2009) Polymer-fullerene bulk-heterojunction solar cells. J Adv Mater 21:1323
47. Schilinsky P, Asawapirom U, Scherf U, Biele M, Brabec CJ (2005) Influence of the molecular weight of poly(3-hexylthiophene) on the performance of bulk heterojunction solar cells. Chem Mater 17:2175
48. Moet DJD, Lenes M, Kotlarskia JD, Veenstra SC, Sweelssen J, Koetse MM, Boer B, Blom PWM (2009) Impact of molecular weight on charge carrier dissociation in solar cells from a polyfluorene derivative. Org Elect 10:1275